Temperature effects on the seismic response in fluid-saturated poroelastic media

*Juan E. Santos * Universidad de Buenos Aires, Facultad de Ingeniería, Instituto del Gas y del Petróleo, School of Earth Sciences and Engineering, Hohai University, Department of Mathematics, Purdue University, Gabriela B. Savioli, Universidad de Buenos Aires, Facultad de Ingeniería, Instituto del Gas y del Petróleo, José M. Carcione, School of Earth Sciences and Engineering, Hohai University, Associate of National Institute of Oceanography and Applied Geophysics, OGS, Trieste, Italy. and Jing Ba, School of Earth Sciences and Engineering, Hohai University*

SUMMARY

The initial boundary-value problem (IBVP)representing the thermo-poroelasticity wave equation is solved applying continuous and discrete-time finite-element (FE) methods. The mathematical model is obtained combining Biot and Lord-Shulman (LS) theories that describe the porous and thermal effects, respectively. The FE methods are formulated on a bounded domain with absorbing boundary conditions at the artificial boundaries. The model predict the propagation of four waves: a fast P wave, a Biot slow wave, a thermal wave, and a shear wave. The solid displacements and the temperature are discretized using globally continuous bilinear polynomials while the fluid displacements is represented by the vector part of the Raviart-Thomas Nedelec of zero order. The theory is illustrated by numerical experiments in a 1D domain. The propagation of the P, slow and thermal waves is shown. We compare the coupled and uncoupled cases, including or neglecting viscosity. The algorithms can be useful for a better understanding of the behavior of seismic waves in hydrocarbon reservoirs and crustal rocks, because the assumption of isothermal wave propagation is now removed.

INTRODUCTION

Falta cambiar y arreglar el tema referencias

Thermoelasticity is the theory that couples the fields of deformation and temperature, where an elastic source gives rise to a temperature field and attenuation and a heat source induces anelastic deformations. The theory is useful in a variety of applications such as seismic attenuation in rocks and material science **???**. The theory might also be relevant in low-temperature physics, theories of shocks and vibrations and astrophysics.

The classical parabolic-type differential equations of thermoelasticity (non-porous) for the Fourier law of heat conduction were reported by Biot **?**, but his theory has unphysical solutions, such as discontinuities and infinite velocities at high frequencies. Later, Lord and Shulman (LS) **?** overcame these problems by formulating a hyperbolic-type differential equations, introducing MVC relaxation times into the heat equation **?**. The thermoelasticity theory predicts and S wave and two P waves, an elastic wave and a thermal wave having similar characteristics to the fast and slow P waves of poroelasticity, respectively **?**. Zener work **?** already contains the concept of mode conversion from P wave to a thermal mode, e.g., he explains P-wave dissipation due to the presence of "microscopic stress inhomogeneities arise from imperfections, such as cavities, and from the elastic anisotropy of the individual crystallites", in the same way that the White model **?** describes attenuation in porous media due to mesoscopic-scale inhomogeneities (as P wave converted to Biot slow mode). Early works in geophysics worth to mention in this sense were conducted by Treitel **?**, Savage **?**, who obtained the P- and S-wave quality factors for empty round cavities or pores, and Armstrong **?**, who considered a finely layered medium. Then, the subject has been neglected in practice till recent works by Carcione and co-workers who performed the first simulation of the thermal wave in the context of thermoelasticity and porothermoelasticity **??????**. In these works, the numerical simulation is performed with a direct method to compute the spatial derivatives, namely, the Fourier pseudospectral differential operator (e.g., **?**). The development of a new technique, based on the FEM algorithm, will provide a more flexible approach to represent the heterogeneities of the medium and will provide further crosscheck of both algorithms and the physics of wave propagation.

Santos and co-workers **?** prove the existence and uniqueness of the Biot/Lord-Shulman formulation in linear thermo-poroelastic isotropic media, with bounded domains under appropriate boundary and initial conditions. The analysis shows the existence of a unique solution, given in terms of displacements of the solid and fluid phases and temperature, and proves its regularity in the space and time variables. The FE spaces used for the spatial discretization of the IBVP are as follows. The components of the solid displacement vector and the temperature are represented by globally continuous piecewise bilinear functions. For the fluid phase, we use locally the vector part of the Raviart-Thomas-Nedelec space of zero order. First, we derive a variational formulation of the continuous-time FE IBVP problem and show the existence and uniqueness of the continuous-time FE solution. Then a priori error estimates are given, which are optimal for the FE spaces used and the assumed regularity of the solution. Finally, explicit and implicit discrete-time FE algorithms are defined, and the conditional stability of the explicit FE procedure is analyzed.

MATHEMATICAL MODEL

We consider a porous medium saturated by a single phase, compressible viscous fluid and assume that the whole aggregate is isotropic. Let θ be increment of temperature above a

reference absolute temperature θ_0 for the state of zero stress and strain.

Let $\mathbf{u} = (\mathbf{u}^s, \mathbf{u}^f)$, where $\mathbf{u}^s = (u_i^s)$ and $\mathbf{u}^f = (u_i^f)$ denote the average particle displacement vectors of the solid and relative fluid phase, respectively. Let $\varepsilon(\mathbf{u}^s) = (\varepsilon_{ij}(\mathbf{u}^s))$ and $\sigma(\mathbf{u},\theta) = (\sigma_{ij}(\mathbf{u},\theta))$ be stress tensors of the solid and bulk material, respectively, and $p_f = p_f(\mathbf{u},\theta)$ be the fluid pressure, with associated constitutive relations

$$\begin{aligned} \sigma_{ij}(\mathbf{u},\theta) = \quad & 2\mu\,\varepsilon_{ij}(u^s) \\ & +\delta_{ij}(\lambda_u \nabla\cdot\mathbf{u}^s + B\nabla\cdot\mathbf{u}^f - \beta\,\theta), \qquad (1) \\ p_f(\mathbf{u},\theta) = \quad & -B\nabla\cdot\mathbf{u}^s - M\nabla\cdot\mathbf{u}^f + \beta_f\theta. \qquad (2) \end{aligned}$$

Biot's dynamical equations taking into account temperature are

$$\begin{aligned} &\rho_b\mathbf{u}^s + \rho^f\mathbf{u}^f - \nabla\cdot\sigma(\mathbf{u},\theta) = \mathbf{f}^s \qquad (3) \\ &\rho^f\mathbf{u}^s + g\mathbf{u}^f + \frac{\eta}{\kappa}\mathbf{u}^f + \nabla p_f(\mathbf{u},\theta) = \mathbf{f}^f, \end{aligned}$$

where $\rho_b = (1-\phi)\rho_s + \phi\rho_f$ denotes the mass density of the bulk material, with ϕ, ρ_s and ρ_f denoting the effecive porosity and mass densities of the solid grains and fluid, respectively). Also, η is the fluid viscosity, κ the permeability and $g = \dfrac{S\rho_f}{\phi}$ the tortuosity.

In (1)-(2) , μ is the dry-rock shear modulus, $\lambda_u = \lambda + \alpha^2 M$, $\alpha = 1 - \dfrac{K_m}{K_s}$, $M = \left(\dfrac{\alpha-\phi}{K_s} + \dfrac{\phi}{K_f}\right)^{-1}$, ϕ is the porosity, $B = \alpha\ M$, $\beta = \beta_m + \beta_f$, with λ_u being the Lamé coefficient of the fluid-saturated frame and K_s, K_m and K_f denoting the bulk moduli of the grains, solid and fluid, respectively. The positive coupling coefficients β_m and β_f are the thermoelasticity coefficients of the frame and fluid, respectively.

On the other hand, the generalized heat equation is (**?**, **?**):

$$\begin{aligned} &\tau\ c\ \ddot{\theta} + c\ \dot{\theta} - \nabla\cdot(\gamma\nabla\theta) + (1-\phi)\beta_m\theta_0\nabla\cdot\dot{\mathbf{u}}^s \\ &+\phi\beta_f\theta_0\nabla\cdot\dot{\mathbf{u}}^f + \tau(1-\phi)\beta_m T_o\nabla\cdot\ddot{\mathbf{u}}^s \qquad (4) \\ &+\tau\phi\beta_f T_o\nabla\cdot\ddot{\mathbf{u}}^f = -q. \end{aligned}$$

where q is a heat source. Also, $\gamma = (1-\phi)\gamma_m + \phi\gamma_f$ is the bulk coefficient of heat conduction (or thermal conductivity), with γ_m and γ_f being the heat conduction of the frame and the fluid, respectively; $c = (1-\phi)c_m + \phi c_f$ is the bulk specific heat of the unit volume in the absence of deformation and τ is a MVC relaxation time. These equations assume thermal equilibrium between the solid and the fluid, i.e., the temperature in both phases is the same. Thermal equilibrium is valid when the interstitial heat transfer coefficient between the solid and fluid is very large and the ratio of pore surface area to pore volume is sufficiently high. Here, we consider β_m, β_f, γ and c as parameters, obtained from experiments or from a specific theoretical model.

A plane wave analysis presented in **?** shows in a thermoporoelastic medium four waves can propagate, a fast (P1) wave, a slow (P2) wave, a thermal (T) wave and a shear (S) wave. The P2 and T waves are diffusive at low frequencies, and the T wave is coupled with both P-waves.

The initial boundary-value problem

The initial boundary-value problem (IBVP) is formulated in an open bounded domain $\Omega \subset R^d$, d=1,2,3 with boundary Γ and a time interval $J = (0,T)$ as follows: find $(\mathbf{u},\theta)$ satisfying (**??**) and (4) with initial conditions

$$\begin{aligned} &\mathbf{u}(x,0) = \mathbf{u}^0 = (\mathbf{u}^{0,s}, \mathbf{u}^{0,f}), \\ &\dot{\mathbf{u}}(x,0) = \mathbf{u}^1 = (\mathbf{u}^{1,s}, \mathbf{u}^{1,f}), \\ &\theta(x,0) = \theta^0, \quad \dot{\theta}(x,0) = \theta^1,\ x \in \Omega, \qquad (5) \end{aligned}$$

and absorbing boundary conditions

$$\begin{aligned} &-\mathscr{G}_\Gamma(\mathbf{u},\theta) = \mathscr{D}\mathscr{S}(\dot{\mathbf{u}}), \\ &-\gamma\nabla\theta\cdot\nu = \tau c v_\theta\dot{\theta} \quad x \in \Gamma, \quad t \in J, \qquad (6) \end{aligned}$$

where

$$\begin{aligned} &\mathscr{G}(\mathbf{u},\theta) = \left(\sigma\nu\cdot\nu, \sigma\nu\cdot\chi, p_f\right)(\mathbf{u},\theta), \\ &\mathscr{S}(\dot{\mathbf{u}}) = \left(\dot{\mathbf{u}}^s\cdot\nu, \dot{\mathbf{u}}^s\cdot\chi, \dot{\mathbf{u}}^f\cdot\nu\right) \qquad (7) \end{aligned}$$

In (6)-(7), ν and χ are the unit vector outer normal and unit vector tangent on Γ oriented counterclockwise. The matrix $\mathscr{D}$ is positive definite and $v_\theta = \sqrt{\gamma/(\tau c)}$ is the heat speed (e.g., Carcione et al.**?**).

An existence and uniqueness result for the solution of (**??**)-(5) with different boundary conditions than those in (6) is given in **?**.

The initial boundary-value problem (**??**)-(6) was solved in the 1D case using a time-explicit conditionally stable Finite Element (FE) method with linear polinomials to represent the temperature and the solid and fluid displacements.

NUMERICAL RESULTS

The IVBP was solved for the 1D case in an interval of 150 m length discretized using a uniform mesh with mesh size $h =$ 0.175 m and a time step $dt = 7.95 \times 10^{-3}$ ms.

The thermoporoelastic material properties are given in Table 1 **?**.

Table 1. Material Properties

Grain bulk modulus, K_s	35 GPa
density, ρ_s	2650 kg/m^3
Frame bulk modulus, K_m	1.7 GPa
shear modulus, μ_m	1.885 GPa
porosity, ϕ	0.3
permeability, k	1 darcy
Fluid bulk modulus, K_f	2.4 GPa
density, ρ_f	1000 kg/m^3
viscosity, η_f	0.001 Pa $\cdot$ s
thermoelasticity coefficient, β_f	40000 kg/(m s^2 K)
Bulk specific heat, c	820 kg/(m s^2 K)
thermoelasticity coefficient, β	120000 kg/(m s^2 K)
absolute temperature, T_0	300 K
thermal conductivity, γ	4.5 $\times 10^6$ kg/m^3
relaxation time, τ	1.5 $\times 10^{-2}$ s

The medium is uniform in all experiments, initially at rest with a point dilatational source $\mathbf{f} = (\mathbf{f}^s, \mathbf{f}^s, q)$ of time history

$$g(t) = -16 f_0^2 (t - t_0) e^{-8 f_0^2 (t-t_0)^2} \tag{8}$$

with $t_0 = 1.25/f_0$ and f_0 being the dominant frequency, chosen to be 200 Hz. At this frequency the approximate values of the phase velocities of P1, P2 and T waves at zero frequency are 2400 m/s, 800 m/s and 500 m/s, respectively.

The source is located at 1 m and temperature and frame and fluid displacements traces are recorded at 61 m.

The experiments consider the uncoupled and coupled Cases considering the vanishing or non-zero coupling coefficients β, β_m and β_f.

Figures 1 and 2 display snapshots of the frame at times 23.5 and 47 ms for the coupled Case and zero viscosity and non-zero viscosities. Figure 1 exhibits clearly the P1, P2 and T waves as they travel along the domain. On the other hand Figure 2 only shows traveling P1 and T waves due to the diffusive behavior of the P2 wave.

Figure 3 compares temperature snapshots at time 23.5 and 47 ms for the uncoupled and coupled Cases for non-zero viscosity. The T wave is seen to travel at lower speed and with much higher amplitude in the coupled than the uncoupled Case. Furthermore in the coupled Case the T wave suffer attenuation when traveling in the domain, while the P1 wave is observed to travel without attenuation.

Figures 4 and 5 displays temperature and frame traces for the coupled Case and zero and non-zero viscosity. As expected, for zero viscosity three wave arrivals are observed (red curve) at early times as compared with the non-zero viscosity curves, where only two arrivals are seen. The T wave is the one with lower amplitude as compared with the P1 and P2 waves.

Finally, Figure 6 shows a frame snapshot at 47 ms for the case when the dilatational source is located only the frame. The additional slowest wavefront corresponds to a T wave generated due to the coupling of the Biot's equation with the heat equation as defined in (3)–(4)

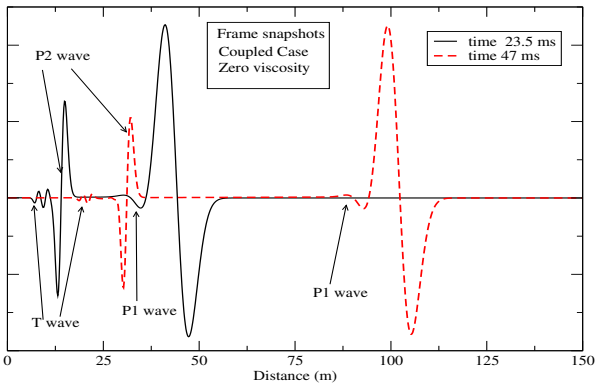

Figure 1: Frame snapshots at 23.5 and 47 ms, coupled Case, zero viscosity case

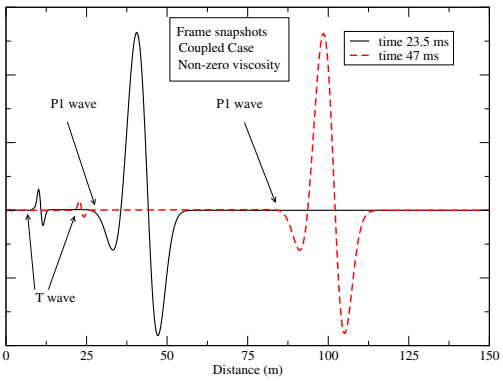

Figure 2: Frame snapshots at 23.5 and 47 ms, coupled Case, non-zero viscosity case

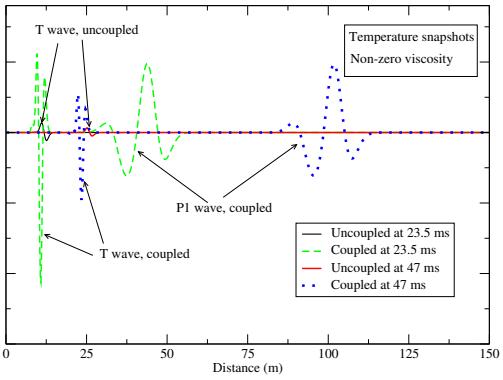

Figure 3: Temperature snapshots, non-zero viscosity case. Comparison between uncoupled and couples Cases at two different times: 23.5 ms and 47 ms

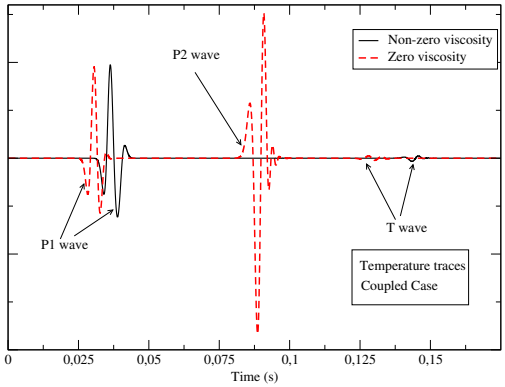

Figure 4: Temperature traces, coupled Case. Comparison between non-zero and zero viscosity cases

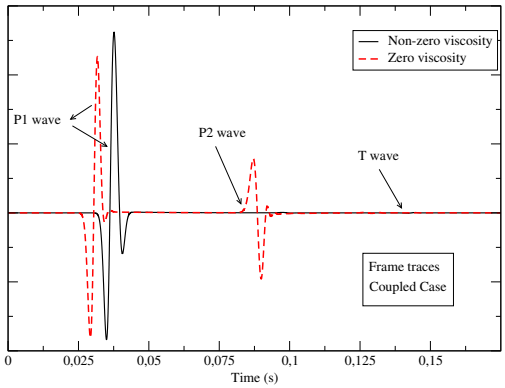

Figure 5: Frame traces, coupled Case. Comparison between non-zero and zero viscosity cases

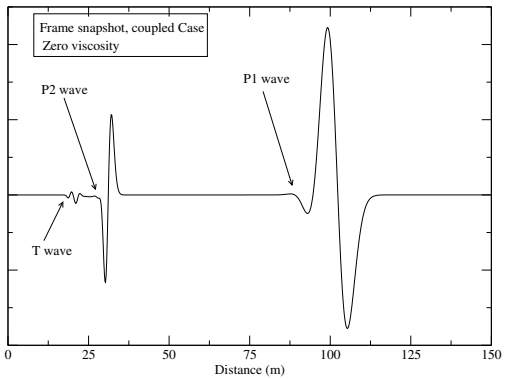

Figure 6: Frame snapshot at 47 ms for zero viscosity. Coupled Case. The source is located only on the frame.

ACKNOWLEDGMENTS

This work was partially funded by ANPCyT, Argentina (PICT 2015 1909) and Universidad de Buenos Aires (UBACYT 20020190100236BA)